Journal of the Mechanical Behavior of Biomedical Materials 78 (2018) 414–419

Contents lists available at ScienceDirect

Journal of the Mechanical Behavior of Biomedical Materials

journal homepage: www.elsevier.com/locate/jmbbm

Polymer matrix of fiber-reinforced composites: Changes in the semi-interpenetrating polymer network during the shelf life

Aftab A. Khan[a,*], Abdulaziz A. Al-Kheraif[a,b], Abdullah M. Al-Shehri[b], Eija Säilynoja[c,d], Pekka K. Vallittu[c,e,1]

[a] Dental Biomaterials Research Chair, College of Applied Medical Sciences, King Saud University, Riyadh, Saudi Arabia
[b] Dental Health Department, College of Applied Medical Sciences, King Saud University, Riyadh, Saudi Arabia
[c] Department of Biomaterials Science, Institute of Dentistry, University of Turku, Turku, Finland
[d] Stick Tech Ltd – Member of GC Group, Turku, Finland
[e] Welfare Division, Turku, Finland

ARTICLE INFO

Keywords:
Fiber-reinforced composite
Resin composite
Monomer
Polymethyl (methacrylate)
Nanohardness
Semi-interpenetrating polymer network

ABSTRACT

This laboratory study was aimed to characterize semi-interpenetrating polymer network (semi-IPN) of fiber-reinforced composite (FRC) prepregs that had been stored for up to two years before curing. Resin impregnated prepregs of everStick C&B (StickTech-GC, Turku, Finland) glass FRC were stored at 4 °C for various lengths of time, *i.e.*, two-weeks, 6-months and 2-years. Five samples from each time group were prepared with a light initiated free radical polymerization method, which were embedded to its long axis in self-curing acrylic. The nanoindentation readings on the top surface toward the core of the sample were made for five test groups, which were named as "stage 1–5". To evaluate the nanohardness and modulus of elasticity of the polymer matrix, a total of 4 slices (100 μm each) were cut from stage 1 to stage 5. Differences in nanohardness values were evaluated with analysis of variance (ANOVA), and regression model was used to develop contributing effect of the material's different stages to the total variability in the nanomechanical properties. Additional chemical and thermal characterization of the polymer matrix structure of FRC was carried out. It was hypothesized that time of storage may have an influence on the semi-IPN polymer structure of the cured FRC. The two-way ANOVA test revealed that the storage time had no significant effect on the nanohardness of FRC ($p = 0.374$). However, a highly significant difference in nanohardness values was observed between the different stages of FRC ($P < 0.001$). The regression coefficient suggests nanohardness increased on average by 0.039 GPa for every storage group. The increased nanohardness values in the core region of 6-months and 2-years stored prepregs might be due to phase-segregation of components of semi-IPN structure of FRC prepregs before their use. This may have an influence to the surface bonding properties of the cured FRC.

1. Introduction

Restorative and prosthetic dentistry has been revolutionized by the use of fiber-reinforced composites (FRCs), which have enabled fabrication of direct and indirect restorations with high mechanical strength and natural looking appearance (Vallittu and Sevelius, 2000; Dyer et al., 2005; Bouillaguet et al., 2006; Garoushi et al., 2006; Xie et al., 2007). Dental FRCs usually consist of reinforcing glass fiber incorporated into a dimethacrylate resin matrix. The glass fibers are silanized to adhere to the resin matrix (Matinlinna et al., 2004). Silane promoted adhesion of glass fibers to the resin matrix is essential for the cohesive strength of the FRC material.

Dental constructs are multiphasic and are composed of FRC substructure and a tooth-colored veneering resin composite layer. In directly made restorations, adhesion of the veneering resin composite or resin luting cement to the surface of FRC substructure can be based on free radical polymerization of the veneering composite to the resin matrix part of the FRC. However, in indirectly made restorations, repairs and luting of FRC root canal posts, the bonding mechanism is typically micromechanical or utilizes exposed glass fiber surfaces. Utilization of exposed glass fibers for bonding the FRC substructure requires chairside silanization, which, however, has proven to be prone to weakening by hydrolysis (Rosen, 1978; Heikkinen et al., 2013; Rosentritt et al., 2001).

* Corresponding author.
E-mail addresses: aakjk@hotmail.com, aftkhan@ksu.edu.sa (A.A. Khan).
[1] Visiting professor King Saud University, Riyadh, Saudi Arabia.

https://doi.org/10.1016/j.jmbbm.2017.11.038
Received 3 July 2017; Received in revised form 4 November 2017; Accepted 22 November 2017
Available online 26 November 2017

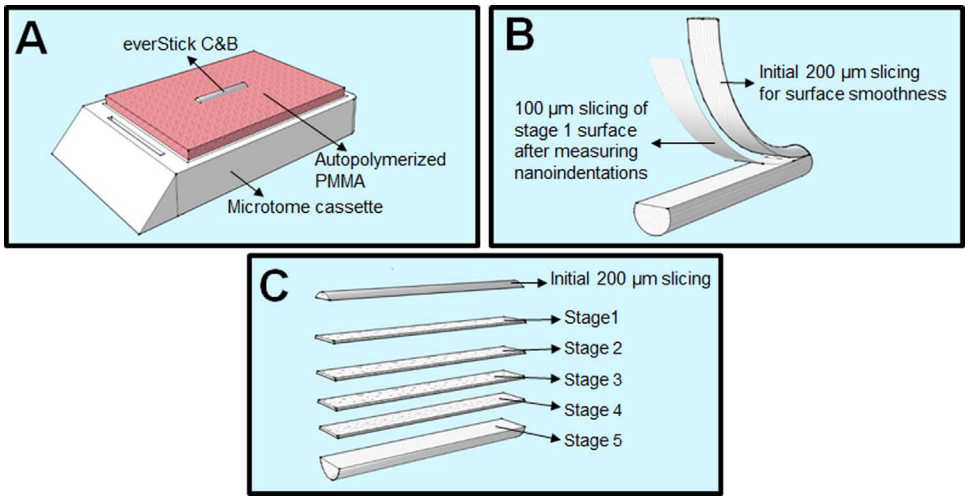

Fig. 1. Sample preparation: (A) 10-mm-long cured FRC sample partially embedded in autpolymerized acrylic resin, (B) Initial 200 µm slicing of the FRC for smoothing of the tested stage 1 surface, (C) Subsequent longitudinal slicing of 100 µm each from stage 1 to stage 5 for nanomechanical and chemical analysis.

Weakening of the bond between the FRC substructure and veneering composite was one of the problems related to early FRC restorations (Bohlsen and Kern, 2003; Goldberg and Freilich, 1999). During the early development of dental FRCs, another approach to adhere veneering resin composites and resin luting cements to the FRC substructure was developed. This approach utilized the polymer matrix of the FRC, which was modified to have lower cross-linking density than that of highly cross-linked dimethacrylate based polymers. A lower cross-linking density was obtained by the addition of monomethacrylate-based macromolecules to the light curing dimethacrylate monomer system and especially to the surface layer of FRC. By definition, the polymer system of poly(methylmethacrylate) (PMMA) and copolymer bisphenol-A-glycidyldimethacrylate–triethylene glycol dimethacrylate (*bis*GMA) is a semi-interpenetrating polymer network (semi-IPN) (Sperling, 1994; Vallittu, 2009; Kallio et al., 2001; Lastumäki et al., 2002). By the International Union of Pure and Applied Chemistry (IUPAC) Comission on Macromolecular Nomenclature, the semi-IPN is *net*-poly(methylmethacrylate)-*inter*-*net*-copoly(bis-glycidyl-A-dimethacrylate)-triethyleneglycol dimethcraylate.

Indeed, the bonding properties of the veneering resin composites and resin luting cements have been shown to improve on using a semi-IPN resin matrix for FRC than a FRC that only has a cross-linked dimethacrylate polymer matrix (Le Bell et al., 2004). The improved bonding was shown to be related to the dissolution of PMMA of the semi-IPN matrix by the monomers of the veneering resin composites or resin luting cements (Mannocci et al., 2005; Wolff et al., 2012; Frese et al., 2014).

The fabrication of semi-IPN containing dental FRC materials (everStick products, Stick Tech-GC, Turku, Finland) enriches the surface of the FRC prepreg with PMMA macromolecules. The prepreg typically comprises continuous unidirectional glass fibers embedded in the resin matrix, ready for molding and curing. PMMA enrichment makes the surface of the FRC less cross-linked and easier to be dissolved by monomers of veneering resin composites in order to enhance interfacial bonding to resin cements and veneering resin composites. Over the shelf life of the FRC prepreg, the resin matrix is in the form of a viscous gel and it can be hypothesized that dimethacrylate monomer diffusion occurs to the PMMA-enriched surface and *vice versa*. The PMMA gradient may therefore change by the storage time, which might have an impact on the bonding properties of the FRC substructure of dental devices and FRC root canal posts of semi-IPN type.

The aim of this study was to characterize nanomechanically, chemically and by thermal means the semi-IPN structure of dental glass FRC prepregs that had been stored for up to two years before curing. More specifically, the surface nanohardness, modulus of elasticity and ratio of PMMA and dimethacrylate copolymers were examined at various depths of the material using Raman spectroscopy and X-ray diffraction. The working hypothesis was that the PMMA gradient would be lower after a longer shelf life period.

2. Materials and methods

A semi-IPN FRC (everStick C&B, StickTech-GC, Turku, Finland) consisting of *bis*GMA, Tri-ethylene-glycol-dimethacrylate (TEGDMA) and PMMA polymer matrix system was selected and the resin impregnated FRC prepregs were stored at 4 °C for various lengths of time, *i.e.*, two-weeks, 6-months, and 2-years. For each storage group, 10 mm of the FRC material was cut off from the fiber frame together with its silicone bedding. Next, the prepreg was polymerized for 5 min in a light curing oven (Labolight LV-III, GC Corporation, Tokyo, Japan) followed by additional 15 min curing in a vacuum oven (Espe Visio® Beta Vario, Espe, Seefeld, Germany) to eliminate oxygen inhibited surface layer.

A self-curing acrylic resin (Rapid Repair, DeguDent GmbH, Hanau, Germany) was selected for embedding the FRC samples for analysis. The acrylic resin was decanted into a tissue-processing cassette, the resin was filled up to 2 mm above the extended sidewalls of the cassette for ease of slicing the samples. Next, a 10 mm polymerized FRC bar was introduced with its length along the horizontal axis in the resin matrix in such a way that half of the diameter (approximately 0.85 mm) of the stick was embedded inside the resin matrix and the remaining half was free from any interaction with the acrylic resin polymer. A single FRC bar was centered in each resin-filled cassette during the sticky stage of polymerization (Fig. 1A). Five samples were prepared for each group *i.e.*, two weeks (Fresh-group), 6-months, and 2-years shelf-life samples. The cured FRC samples were stored in a desiccator for 48 h before any further process or analysis were undertaken.

2.1. Nanoindentation tests

Nanoindentations of the polymer matrix phase of the FRC were obtained with a nano-mechanical tester (Bruker, Santa Barbara, CA, USA) equipped with a Berkovich diamond indenter tip with nominal radius ≈100 nm. To obtain an accurate indenter area function and ensure instrument compliance, the system was calibrated using a fused silica block with E = 72 GPa. The experiments were performed at a controlled temperature of 26 °C ± 1 °C, with loading and unloading rates of 0.05 mN/s and a 10 s dwell time. The maximal load was set to 0.5 mN (Fig. 2).

Initially, each FRC bar was sectioned 200 µm longitudinally along its long axis with a microtome saw (SLEE CUT 5062, SLEE Medical, Mainz, Germany) to provide a smooth and even surface for nanoindentation of the polymer matrix (Fig. 1B). During testing, the

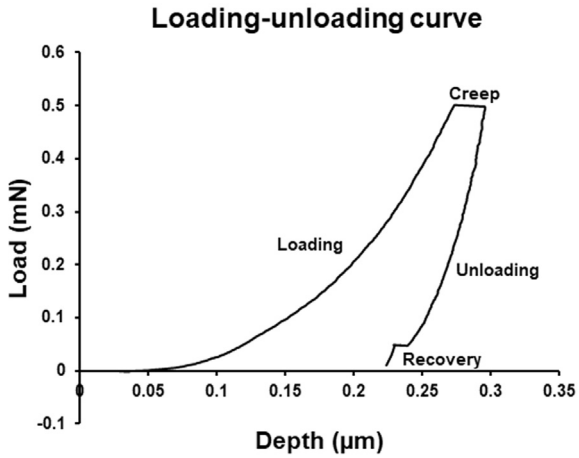

Fig. 2. Schematic representation of a loading-unloading curve for a nanoindentation measurement of the polymer matrix of semi-IPN FRC.

indenter (three-sided pyramidal Berkovich diamond tip, 100 nm radius) was pressed randomly onto the sample's polymer matrix surface (between the fibers). On each sample, 5 indents were made at least 50 μm apart to avoid overlapping of the indentations. The nanoindentations being introduced on the top surface of each sample from the tested groups comprised “stage 1.” Next, with a microtome saw, a 100-micron slice was cut longitudinally from everStick C&B bar and evaluated for 5 nanoindents. This stage of evaluation was named “stage 2”. The nanoindentation evaluation of “stage 3” was performed by cutting 100 μm off once again. To evaluate the nanomechanical properties (nanohardness and modulus of elasticity) of the polymer matrix, 4 slices (100 μm each) were cut from stage 1 to stage 5.

2.2. Raman spectroscopy

Raman spectra of the top (stage 1) and the core (stage 5) surfaces were acquired using a ProRaman-L Analyzer (TSI®, Shoreview, MN, USA) with an excitation laser beam wavelength of 785 nm. The scanning was undertaken between 250 and 2350 cm^{-1}. However, special emphasis was made with the scanning at 1450 cm^{-1} and 1640 cm^{-1} to evaluate the structural fingerprints of PMMA and *bis*GMA, respectively.

2.3. X-ray diffraction (XRD) analysis

XRD patterns of stage 1 and stage 5 surfaces of the polymer matrix were determined using a D-8 Discover X-ray diffractometer (Bruker AXS GmbH, Oestliche Rheinbrueckenstr, Karlsruhe, Germany) in the 2θ range of 30–90°, at a scan speed of 2°/min with an increment of 0.02 in locked coupled mode.

2.4. Thermographic analysis

Thermogravimetric analysis (TGA) and differential scanning calorimetry (DSC) were estimated using SDT Q600 (TA Instruments, New Castle, DE, USA). The glass-transition temperature (T_g) of the polymer matrix of stage 1 and stage 5 of the FRC was estimated separately. For thermal analysis, individual samples (approximately ⌀ 1.7 mm, L = 5 mm, and weight in the range of 5.80–6.26 mg) were placed in an alumina pan inside the heating compartment, and then the sample was heated at 10 °C/min from 23 °C to 600 °C under a nitrogen environment. The acquired data were evaluated through the software fitted in Q600.

2.5. Statistical analyses

Statistical analyses were achieved using SPSS ver. 23.0 (Statistical Package for Social Science, SPSS Inc., Chicago, IL; USA). All data were confirmed for the normality of their distribution using the Shapiro-Wilk test and Kolmogorov–Smirnov test ($\alpha = 0.05$). Levene's test was carried out for the homogeneity of variance. Descriptive data and inferential data such as the regression model was used to explore the relationship between the nanohardness and different surface stages of the FRC samples. Subsequently, analysis of variance (ANOVA) was used to test for differences within and between the sample groups (*post hoc* Tukey's test = 0.05).

3. Results

Table 1 presents the descriptive data for the nanohardness values along with the statistical differences within and between the tested groups at different stages. The two-way ANOVA test revealed that the storage condition had no significant effect on the nanohardness of FRC ($P = 0.374$). However, a highly significant difference in nanohardness values was observed between the different stages of FRC ($P < 0.001$). Further, the interaction (joint effect) of storage condition and material's different stages was also found to be significant ($P = 0.001$). The *post hoc* Tukey's test revealed no significant difference within the Fresh-group. However, there was statistical difference within the groups stored for 6-months and 2-years groups and between the groups. Table 2 presents the corresponding values for modulus of elasticity. Modulus of elasticity was lower at stage 1, *i.e.*, at the surface of the FRC than in the core. By lengthening the storage time, the difference between the modulus of elasticity at the surface compared to the core became more evident. In fact, the highest modulus of elasticity was found with the FRC, which was cured from a prepreg with 2-year storage.

The regression analysis showed that the contributing effect of the material's different stages to the total variability in the nanohardness was low ($R^2 = 0.2$). However, the regression coefficient was observed to be significant (0.039, $P = 0.000$). Fig. 3 demonstrates the relationship between the storage condition of the FRC samples and the nanohardness of the polymer matrix at different stages.

All samples were analysed by Raman dispersive spectroscopy (Fig. 4) in order to determine the effect of storage conditions of the prepreg on polymer matrix characteristics. The Raman spectra show bond deformation of C-C-O and C-C-C at 500 cm^{-1}. Peaks observed in

Table 1
The mean nanohardness values of polymer matrix of FRC stored for various lengths of time before curing. Stages 1–5 refer to the depth of the measurement from the surface toward core of the material.

Storage condition	Nanohardness (GPa)				
	Stage 1	Stage 2	Stage 3	Stage 4	Stage 5
Fresh	$0.12 \pm 0.03_{a,b}$	$0.13 \pm 0.04_{d,e}$	0.13 ± 0.07	0.17 ± 0.09	0.17 ± 0.09
6-months aged	$0.08 \pm 0.05^{A,B}_{a,c}$	$0.08 \pm 0.05^{C,D}_{d}$	0.13 ± 0.10^{E}	$0.19 \pm 0.12^{A,C,F}$	$0.29 \pm 0.18^{B,D,E,F}$
2-years aged	$0.06 \pm 0.02^{G}_{b,c}$	$0.07 \pm 0.03^{H}_{e}$	0.13 ± 0.09^{I}	0.14 ± 0.11^{J}	$0.28 \pm 0.24^{G,H,I,J}$

Key: Same superscript uppercase letters demonstrate significant difference within the group ($p < 0.05$). Same subscript lowercase letters demonstrate significant difference between the groups ($p < 0.05$).

Table 2
The mean modulus of elasticity values of polymer matrix of FRC stored for various lengths of time before curing. Stages 1–5 refer to the depth of the measurement from the surface toward core of the material.

Storage condition	Modulus of elasticity (GPa)				
	Stage 1	Stage 2	Stage 3	Stage 4	Stage 5
Fresh	$2.49 \pm 0.18^{A,B,C,D}_{a}$	$2.99 \pm 0.24^{A,E,F}_{c,d}$	$2.81 \pm 0.19^{B,G,H}_{e}$	$3.50 \pm 0.29^{C,E,G}_{g,h}$	$3.58 \pm 0.32^{D,F,H}_{j,k}$
6-months aged	$2.19 \pm 0.23^{I,J,K}_{a,b}$	$2.22 \pm 0.28^{L,M,N}_{c}$	$2.93 \pm 0.41^{I,L,O,P}_{f}$	$4.26 \pm 0.79^{J,M,O,Q}_{g,i}$	$5.62 \pm 1.27^{K,N,P,Q}_{j,l}$
2-years aged	$2.51 \pm 0.54^{R,S,T}_{b}$	$2.26 \pm 0.63^{U,V,W}_{d}$	$5.73 \pm 1.09^{R,U,X}_{e,f}$	$6.14 \pm 1.81^{S,V,Y}_{h,i}$	$8.28 \pm 2.19^{T,W,X,Y}_{k,l}$

Key: same superscript uppercase letters demonstrate significant difference within the group ($p < 0.05$). Same subscript lowercase letters demonstrate significant difference between the groups ($p < 0.05$).

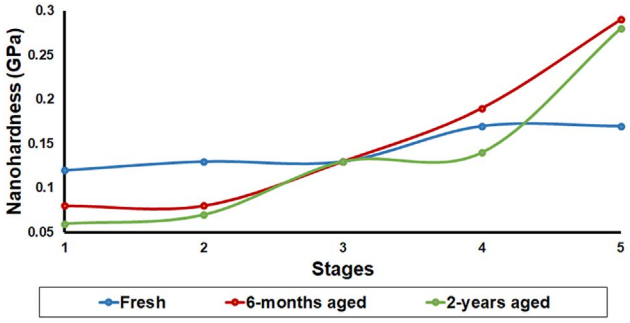

Fig. 3. Nanohardness of the polymer matrix cured from fresh, 6-months, and 2-years stored FRC prepregs, plotted against the depth of the measurement (stages 1–5) from the surface toward core of the FRC.

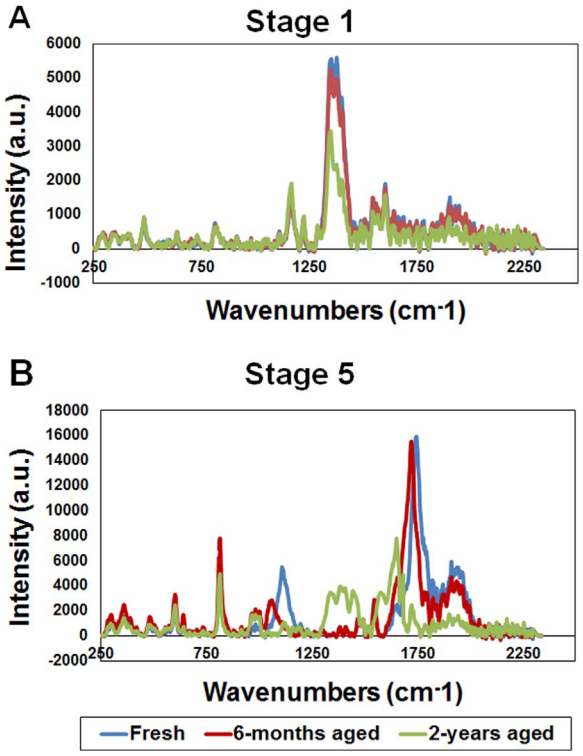

Fig. 4. Raman spectra of polymer matrix: (A) surface of "stage 1" and (B) surface of "stage 5" of the FRC cured from prepregs and stored for various lengths of time.

the range from 730 to 850 cm^{-1} are related to Si-O stretching (Khan et al., 2017). In each tested group the core of the FRC demonstrated an increased intensity (in the range from 1600 to 1750 cm^{-1}) when compared to corresponding top surface of the group. Asymmetric and symmetric deformation in the plane of CH_2 was observed on the top surface in all the groups in the range of 1350–1450 cm^{-1}. The aromatic and aliphatic C=C bond and C=O bond bands were observed in range of

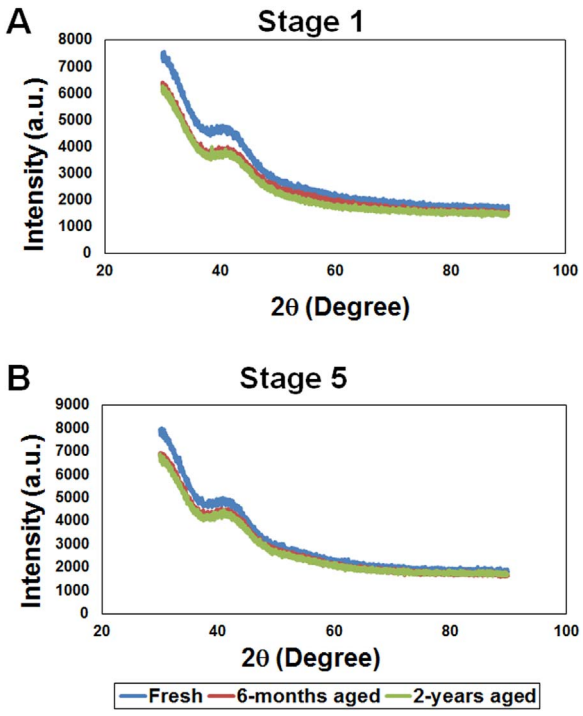

Fig. 5. X-ray diffraction patterns: (A) surface of "stage 1" and (B) surface of "stage 5" of the FRC cured from prepregs and stored for various lengths of time.

1650–1750 cm^{-1}.

The X-ray diffraction patterns of the polymer matrix of stage 1 and stage 5 of the polymer matrix of the FRC suggested that the polymer was amorphous without having a long-range atomic order. Only a broad scattering peak ($2\theta = 40$) was observed in every tested group. Fig. 5 presents the XRD patterns of the tested groups.

Fig. 6 presents the thermal stability of stage 1 and stage 5 of the tested groups. The TGA curves suggest that the top surface (stage 1) of all the tested materials stored for various lengths of time started weight loss at 320 °C. By the time temperature reached to 420 °C, the polymeric weight content was completely lost. However, no weight changes were observed in glass-fiber content. Similar trend was also witnessed for the core surfaces of the tested groups.

Fig. 7 shows the DSC curves of the tested groups. The data suggest that no significant effect to the melting temperature of the tested samples occurred when the surfaces were without monomer interaction at stage 1 (top surface) or with the monomer interaction at stage 5 (core surface). The Tg values from the inserts suggest approximately 200 °C for all the groups.

4. Discussion

Resin-based dental materials have a limited shelf life due to a potential risk for evaporation of monomers, initiator and activator

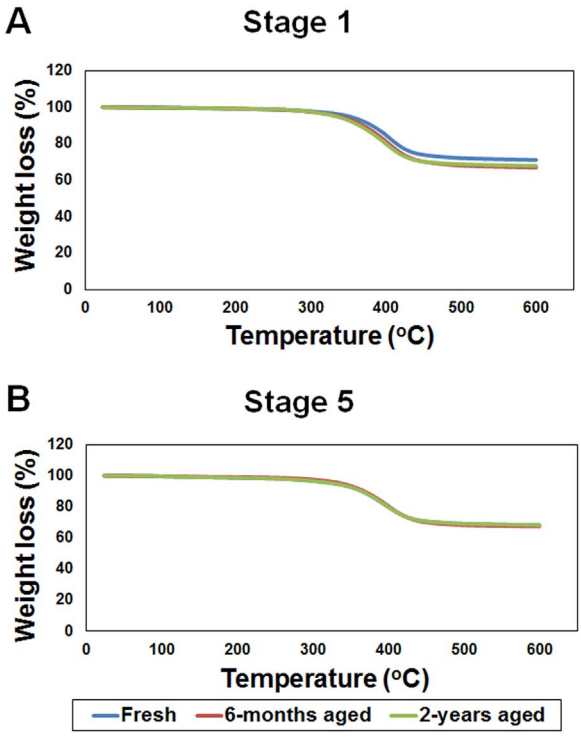

Fig. 6. TGA curves: (A) surface of "stage 1" and (B) surface of "stage 5" of the FRC cured from prepregs and stored for various lengths of time.

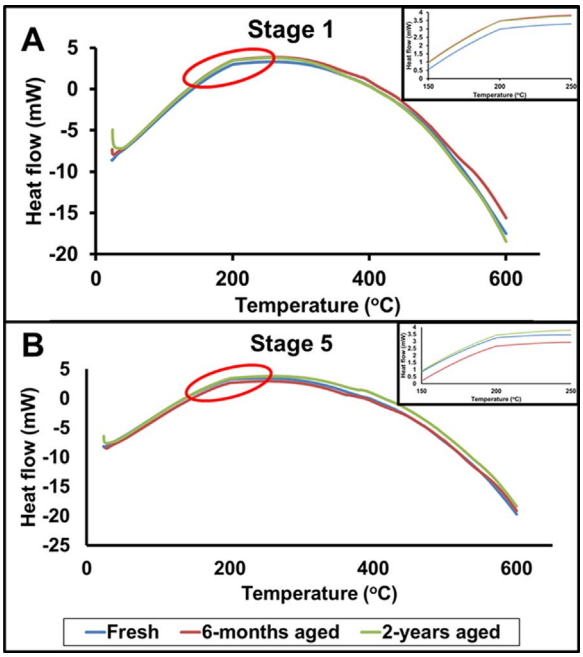

Fig. 7. DSC thermograms depicting heat flow at: (A) surface of "stage 1" and (B) surface of "stage 5" of the FRC cured from prepregs and stored for various lengths of time.

compounds. Until to the introduction of semi-IPN FRCs, there has not been a need to study potential change of the polymer structure in terms of *e.g.* cross-linking density of the polymer matrix, which is known to have an impact on the adhesive properties of the FRC (Kallio et al., 2001; Lastumäki et al., 2002; Le Bell et al., 2004; Mannocci et al., 2005). Change of the polymer structure could occur due to intentionally produced resin gradient structure of the semi-IPN, where there is an enriched layer of PMMA on the surface of the FRC prepreg. Gradient structure may be changed by time from that of fabrication of the FRC prepregs. The change could be due to diffusion of cross-linking monomers and dissolved PMMA molecules. Methods to investigate indirectly the changes of the polymer structure and cross-linking density is based on mechanical means, which in this study were nanomechanical analysis of the polymer matrix. The selected background variables were fresh *versus* two years stored FRC prepregs. The focus was on the differences at the surface layer and in the core of the FRC, especially in terms of surface nanohardness and modulus of elasticity, which relates to the cross-linking density. Characterization of a material through hardness is an important step (Sattler, 2010). However, nanoindentation is a useful technique to measure the unit area of the indented surface at nanoscale (Sattler, 2010). The presence of molecules of PMMA in the cross-linked polymer network lowered the cross-linking density and could be perceived in the values of hardness and elasticity.

The nanoindentation data of this study are indeed interesting and against the hypothesis that the PMMA gradient will be lower after a longer shelf life period. We found that both surface nanohardness and modulus of elasticity were lower in the polymer matrix of the surface layer than in the core of the FRC. This confirms that during the fabrication process of FRC prepregs of this brand, higher quantities of PMMA is present in the core. Although, no visual difference in hue and colour of the prepegs of the tested groups was observed during fabrication. In laboratory studies, this gradient structure has been shown to influence the dissolving characteristics and the adhesion properties of the FRC (Mannocci et al., 2005; Wolff et al., 2012). Interestingly, it was found that when the FRC was cured from the prepreg, which had stored up to two years before curing, the difference of the nanohardness and modulus of elasticity became even higher when the surface and core of the FRC were compared (Tables 1 and 2). In fact, the modulus of elasticity of the core, where there was initially also minor quantities of PMMA, reached at two years storage time the modulus of elasticity of cross-linked *bis*GMA-TEGDMA polymer (Pastila et al., 2007). Surface nanohardness measurement supports also understanding that cross-linking density in the core is higher in FRC made of prepregs of longer storage time. This finding suggests that the PMMA molecules concentrate by diffusion even more to the core of the FRC prepreg when the storage time prolonged (Fig. 3). Consequently, the semi-IPN of this composition is heterogeneous phase-separated material where polymers are dual-phase at molecular level (Sperling, 1981). When thermodynamic interaction between polymer components, kinetic motion, and mobility of polymer chain take place during diffusion, phase-segregation between the network chains may expedite, as found in this study (Sperling, 1981). This unpredictable behavior might be due to relatively limited stability of polymer components of this particular semi-IPN, resulting into disintegration of dual-phases with aging of the FRC prepreg.

This study made an initial attempt to chemically characterize the polymer structure of the FRC which has semi-IPN polymer matrix. By chemical analysis, it was possible to identify the structural differences between the top surface and the core surface, namely PMMA and a major component of di-methacrylate, *i.e.*, *bis*GMA. The core of the FRC demonstrated an increased intensity in the range from 1600 to 1750 cm^{-1} that have the characteristic Raman bands related to aromatic rings, thus it seems obvious that core is *bis*GMA rich. Surface spectra, on the other hand, showed very weak interaction, revealing the existence of PMMA rich layer (Fig. 4). The slight differences in core spectra of Fresh and 2-year sample need to be studied further in order to fully explain the differences observed.

However, it was not possible to see any other structural changes, *i.e.*, crystallization over storage time. XRD analysis showed broad diffraction peaks related to amorphous glass in every time point and in both measuring stages (Fig. 5). This differs from the results with particulate filler resin composite, where crystallinity of the resin composite was found (D'Alpino et al., 2014). However, if the resin composite was used after the expiration date, the crystallinity was less. On the other hand, the major component of the semi-IPN polymer is thermoset of *bis*GMA and TEGDMA, and thermosets are known to be typically

amorphous due to crosslinks, which inhibit the movement of polymer chains to crystallize. Therefore, if the crystallinity or semi-crystallinity would have been noticed, that would probably be in the thermoplastic PMMA phase of the semi-IPN polymer. Although we did not found crystallinity of PMMA, it has been shown that PMMA have ability to crystallize, especially isotactic PMMA (Ute et al., 1995). Amorphous polymer structure of PMMA could be explained also by the PMMA used in this particular semi-IPN system, which is predominantly syndiotactic with a lower tendency for crystallization (Ruyter and Svendsen, 1980). TGA test showed no differences in degradation between core and surface (Fig. 6). The degradation began around 290 °C and above 440 °C the sample mass tended to stabilize, corresponding to glass fiber inorganic content. DSC test further revealed no unusual thermal events *e.g.* crystallization, change in melting or glass transition temperature between core and surface of all tested groups (Fig. 7). These results reflect behavior of predominant thermoset components of the semi-IPN.

Since this study testified improved nanohardness inside the core of the 6-months and 2-years aged samples, further studies are required to analyse the interfacial bond strength with the adhesives. For future studies, it would be interesting to evaluate the effect of storage temperature on resin impregnated FRC prepregs. Since polymers of different compositions may need certain temperature to remain in stable state, and abstaining from entanglement of small chains. Therefore, influence of storage temperature is necessary to explore.

5. Conclusion

This laboratory study demonstrated that:

- The semi-IPN structure of everStick C&B is affected by the long-term storage of FRC prepreg before curing.
- The intentionally fabricated PMMA enrichment on the surface of the FRC prepreg becomes even higher gradient like polymer structure by storing the prepregs for up to two years.
- The polymer matrix of the semi-IPN FRC becomes lower in nanohardness and modulus of elasticity on the surface than in the core by the long-term storage of FRC prepreg before curing.

Acknowledgement

The authors are grateful to the Deanship of Scientific Research, King Saud University for funding through the Vice Deanship of Scientific Research Chairs. Authors express their thanks to Stick Tech – GC for providing the study material.

References

Bohlsen, F., Kern, M., 2003. Clinical outcome of glass-fiber-reinforced crowns and fixed partial dentures: a three-year retrospective study. Quintessence Int. 34, 493–496.
Bouillaguet, S., Schutt, A., Alander, P., Vallittu, P.K., Schwaller, P., Buerki, G., Michler, J., Cattani-Lorente, M., Krejci, I., 2006. Hydrothermal and mechanical stresses degarde fiber-matrix interfacial bond strength in dental fiber-reinforced composites. J. Biomed. Mater. Res B - Appl. Biomater. 76, 98–105.
D'Alpino, P.H., Vismara, M.V., González, A.H., de Oliveira, Graeff, C.F., 2014. Free radical entrapment and crystallinity of resin composites after accelerated aging as a function of the expiration date. J. Mech. Behav. Biomed. Mater. 36, 82–89.
Dyer, S.R., Lassila, L.V.J., Alander, P., Vallittu, P.K., 2005. Static strength of molar region direct technique glass-fibre-reinforced composite fixed partial denture. J. Oral. Rehabil. 32, 351–357.
Frese, C., Decker, C., Rebholz, J., Stucke, K., Staehle, H.J., Wolff, D., 2014. Original and repair bond strength of fiber-reinforced composites in vitro. Dent. Mater. 30, 456–462.
Garoushi, S.K., Ballo, A.M., Lassila, L.V.J., Vallittu, P.K., 2006. Fracture resistance of fragmented incisal edges restored with fiber-reinforced composite. J. Adhes. Dent. 8, 91–95.
Goldberg, A.J., Freilich, M.A., 1999. An innovative pre-impregnated glass fiber for reinforcing composites. Dent. Clin. N. Am. 43, 127–133.
Heikkinen, T.T., Matinlinna, J.P., Vallittu, P.K., Lassila, L.V., 2013. Long term water storage deteriorates bonding of composite resin to alumina and zirconia short communication. Open Dent. J. 7, 123–125.
Kallio, T., Lastumäki, T., Vallittu, P.K., 2001. Bonding of restorative composite resin to some polymeric composite substrates. Dent. Mater. 17, 80–86.
Khan, A.S., Khalid, H., Sarfraz, Z., Khan, M., Iqbal, J., Muhammad, N., Fareed, M.A., Rehman, I.U., 2017. Vibrational spectroscopy of selective dental restorative materials. Appl. Spectrosc. Rev. 52, 507–540.
Lastumäki, T.M., Kallio, T.T., Vallittu, P.K., 2002. The bond strength of light-curing composite resin to finally polymerized and aged glass fiber-reinforced composite substrate. Biomaterials 23, 4533–4539.
Le Bell, A.-M., Tanner, J., Lassila, L.V.J., Kangasniemi, I., Vallittu, P.K., 2004. Bonding of composite resin luting cement to fibre-reinforced composite root canal post. J. Adhes. Dent. 6, 319–325.
Mannocci, F., Sheriff, M., Watson, T.F., Vallittu, P.K., 2005. Penetration of bonding resins into fiber posts: a confocal microscopic study. Endodont. J. 38, 46–51.
Matinlinna, J.P., Areva, S., Lassila, L.V., Vallittu, P.K., 2004. Characterization of siloxane films on titanium substrate derived from three aminosilanes. Surf. Interface Anal. 36, 1314–1322.
Nanoindentation of biomaterials, 2010. In: Sattler K.D. (Ed.), Handbook of Nanophysics: Functional Nanomaterials. Boca Raton: CRC Press.
Pastila, P., Lassila, L.V., Jokinen, M., Vuorinen, J., Vallittu, P.K., Mäntylä, T., 2007. Effect of short-term water storage on the elastic properties of some dental restorative materials - a resonant ultrasound spectroscopy study. Dent. Mater. 23, 878–884.
Rosen, M.R., 1978. From treating solution to filler surface and beyond-life-history of a silane coupling agent. J. Coat. Tech. 50, 70–82.
Rosentritt, M., Behr, M., Kolbeck, C., Handel, G., 2001. In vitro repair of three-unit fiber-reinforced composite FPDs. Int J. Prosthodont. 14, 344–349.
Ruyter, I.E., Svendsen, S.A., 1980. Flexural properties of denture base polymers. J. Prosthet. Dent. 43, 95–104.
Sperling, L.H., 1981. An Introduction to Polymer Networks and IPNs. Interpenetrating Polymer Networks and Related Materials. Plenum Press, New York.
Sperling, L.H., 1994. Interpenetrating polymer networks: an overview. Advances in chemistry. ACS publications, Washington DC.
Ute, K., Yamasaki, Y., Naito, M., Miyatake, N., Hatada, K., 1995. Controlled synthesis of isotactic and symmetrical poly (methyl methacrylate) directed toward uniform polymers with high crystallinity. Polym. J. 27 (9), 951–958 (Sep 1).
Vallittu, P.K., 2009. Interpenetrating polymer networks (IPNs) in dental polymers and composites. J. Adhes. Sci. Technol. 23, 961–972.
Vallittu, P.K., Sevelius, C., 2000. Resin-bonded, glass fiber-reinforced composite fixed partial dentures: a clinical study. J. Prosthet. Dent. 84, 413–418.
Wolff, D., Geiger, S., Ding, P., Staehle, H.J., Frese, C., 2012. Analysis of the interdiffusion of resin monomers into pre-polymerized fiber-reinforced composites. Dent. Mater. 28, 541–547.
Xie, Q., Lassila, L.V.J., Vallittu, P.K., 2007. Comparison of load-bearing capacity of direct resin-bonded fiber-reinforced composite FPDs with four framework designs. J. Dent. 35, 578–582.